Synchronization in a ring of four mutually coupled van der Pol oscillators: Theory and experiment

B. Nana and P. Woafo*
Laboratory of Nonlinear Modelling and Simulation in Engineering and Biological Physics, Faculty of Science, University of Yaounde I, Box 812 Yaounde, Cameroon
(Received 2 January 2006; published 24 October 2006)

We investigate different states of synchronization in a ring of four mutually coupled van der Pol oscillators. The stability analysis and numerical simulation are performed to determine the suitable coupling parameters leading to high-quality synchronization. The consequences of parameter mismatch are also highlighted. Experimental realization is then used to show the existence of complete and partial synchronization.

DOI: 10.1103/PhysRevE.74.046213 PACS number(s): 05.45.Xt

I. INTRODUCTION

The synchronization of chaotic oscillators has gathered increasing interest during this past decade [1–4]. Complete synchronization of chaotic oscillators has been described theoretically and observed experimentally. With radio and electronics development in this view, synchronization occupies a very special place in science and technology. As many phenomena studied in nonlinear dynamics, synchronization was observed and shown to play an important role in many problems of diverse natures: physical, ecological, physiological, meteorological, biological, to name a few. There is hardly a single communication or data storage application that does not rely on synchronization [5–7]. Consequently, intense research activities are actually conducted for the synchronization of electronic oscillators which are currently the standard electronic emitter-receiver systems.

Another field where synchronization is of particular interest is the biological science. This is, for instance, the case of coupled cells (each cell is composed of a set of neurons directly responsible to harmonize the movement of the leg) activated by the locomotion central pattern generator (CPG) for bipeds and quadrupeds. This system has been intensively studied by various authors [8–13]. The main results so far obtained are the following: (i) There are some remarkable parallels between the generalities of coupled nonlinear oscillators and the observed symmetries of gaits [8]; (ii) the network of symmetrically coupled cells described by coupled ordinary differential equations exhibits the quadruped gaits of walk, trot, and pace, with the primary gaits having been produced from Hopf bifurcation by varying only the coupling strengths of the network [9–11]; (iii) heteroclinic cycles also occur in rings of coupled cells [12]; and (iv) the network, with and without delay diffusive interactions, in the chaotic state can describe a number of natural gaits as well as some which are known to be learned [13]. See Ref. [14] (and references therein), where a general review of the major ideas involved in the field of synchronization of chaotic systems has been reported with their relevance in physiology, nonlinear optics, and fluid dynamics, including experimental applications.

Recently, by using the averaging method, Ookawara and Endo [15] proved that for a ring of three coupled oscillators, two frequencies bifurcate from the degenerate mode, synchronize if they are close enough, but lose synchronization when they are separated to a certain extent. However, for a ring of four coupled oscillators, the two frequencies generally cannot be synchronized, even if they are close enough. Lately, Woafo and Enjieu Kadji [16] studied the synchronized states in a ring of mutually coupled self-sustained electrical oscillators described by the coupled van der Pol equations. After using the Floquet theory and the Whittaker method to analyze the stability of the synchronization in the ring, they analyzed the effect of local injection strength on the behavior of the ring.

The purpose of this paper is to determine the synchronized states in a ring of four mutually coupled nonidentical van der Pol oscillators both in their regular and chaotic states. The approach that we will follow in the analysis lies in the context of the qualitative theory of nonlinear dynamical systems [17]. We emphasize that, in general, nonlinear dynamical systems cannot be solved analytically, thus recourse to numerical simulations. Even with the numerical simulations, one does not have a complete understanding of real behavior of the devices. It is therefore important to realize systems experimentally to expect a more complete understanding. Recently, following the results of Ref. [5], Heisler *et al.* [18] investigated experimentally the partial synchronization in a ring of six diffusively coupled Rössler circuits with different coupling schemes. They found the partial synchronization and other patterns predicted by the analysis of the symmetries of the ring. The differences with the present study appear not only on the type of oscillators but also on the points analyzed, since we consider both the autonomous and nonautonomous cases and investigate the range of coupling parameters and external forces for good quality synchronization.

The paper structure is as follows. In Sec. II, the analytical and numerical studies of the stability of the synchronization process are presented and discussed. In Sec. III, we present the experimental implementation; the experimental results are compared to those obtained numerically and analytically.

*Corresponding author: pwoafo@uycdc.uninet.cm

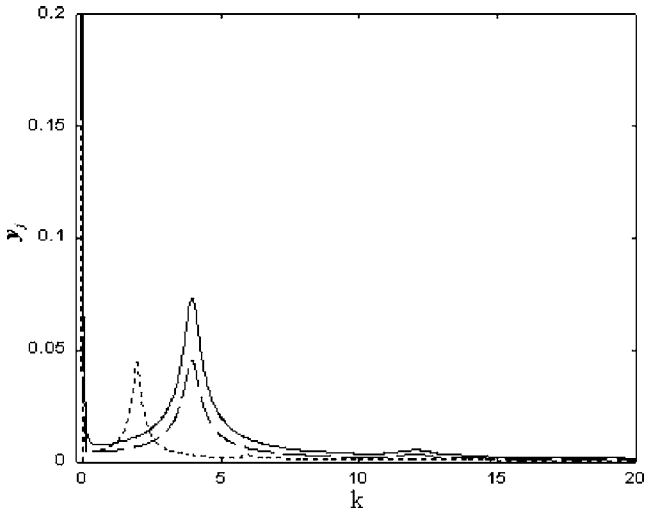

FIG. 1. Maximal values taken by the three modes y_1 (full line), y_2 (dashed), and y_3 (dotted).

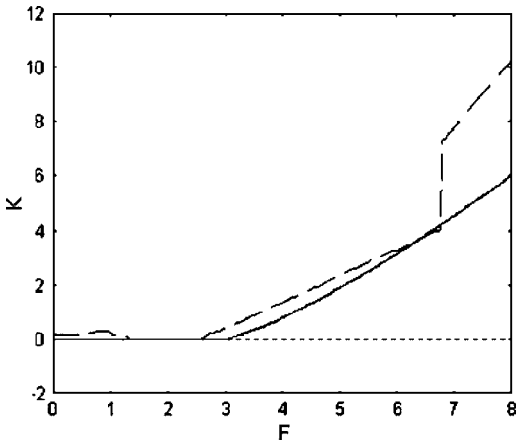

FIG. 2. The coupling coefficient boundary for complete synchronization vs the amplitude F of the external excitation for d_j=0.31. Full line shows analytical result and dashed line shows numerical result.

The last section is devoted to the conclusion. Numerical simulation of all ordinary differential equations makes use of the fourth-order Runge-Kutta algorithm.

II. MODEL AND THEORETICAL ANALYSIS

A. The model

We consider a ring of four mutually coupled van der Pol oscillators described by the following second-order dimensionless nonlinear differential equations:

$$\ddot{x}_1 - d_1(1-x_1^2)\dot{x}_1 + x_1 = k_1(x_4 - 2x_1 + x_2) + F_1 \cos \Omega t,$$

$$\ddot{x}_2 - d_2(1-x_2^2)\dot{x}_2 + x_2 = k_2(x_3 - 2x_2 + x_1) + F_2 \cos \Omega t,$$

$$\ddot{x}_3 - d_3(1-x_3^2)\dot{x}_3 + x_3 = k_3(x_2 - 2x_3 + x_4) + F_3 \cos \Omega t,$$

$$\ddot{x}_4 - d_4(1-x_4^2)\dot{x}_4 + x_4 = k_4(x_1 - 2x_4 + x_3) + F_4 \cos \Omega t. \quad (1)$$

The dot over each quantity denotes its time derivative. d_1, d_2, d_3, and d_4 are positive coefficients. They measure the dissipative strength because if $|x_j|$ $(j=1,2,3,4)$ is smaller than 1, the system experiences negative damping and its amplitude increases; otherwise, the damping causes the amplitude to decrease. So the entire phase plane is a basin of attraction for the stable limit cycle. Thus the nonlinear terms play the role of amplitude-dependent dissipation and provide a self-sustaining mechanism for the perpetual oscillation. k_1, k_2, k_3, and k_4 are coupling coefficients. Our choice of considering nonidentical coefficients is justified by the parameter mismatches encountered in real systems. F_i and Ω are the amplitudes and frequency of the external excitations.

Equations (1) are interesting because they model several phenomena and have applications in many domains. For example, this model is mainly used in electronic engineering as a network of parallel microwave oscillators. Such a network helps to investigate the possibility of simultaneous multimode oscillations and accordingly, the stability of several nonresonant modes of oscillations under specific boundary conditions (see Ref. [15] and references therein). In biology, the network of a large number of these oscillators can be used to model intestinal signals or colorectal myoelectrical activity in humans [17,19].

B. Theoretical results for the ring without external excitations

The case of identical oscillators has been solved analytically and numerically in Ref. [16]. It was found that in the autonomous case where F_i=0 $(i=1,2,3,4)$ and identical coupling $k_i=k$, the modes $y_2=x_4-x_2$, $y_3=x_3-x_1$, and $y_1=x_4-x_3+x_2-x_1$ go to zero for $k \in [-0.25; -0.0011] \cup [0.004; +\infty]$. Thus the ring is said to be in the complete synchronization state where $x_1 \cong x_2 \cong x_3 \cong x_4$. Figure 1 shows that this complete synchronization state can be obtained even in the case of oscillators having slightly different coefficients. The figure shows the maximal values of $|y_2|$, $|y_3|$, and $|y_1|$ when k varies with $k_1=0.2+k$, $k_2=0.21+k$, $k_3=0.199+k$, and $k_4=0.214+k$, and $d_1=0.2$, $d_2=0.21$, $d_3=0.22$, and $d_4=0.198$.

C. Theoretical results for a ring with external excitations

The aim of this section is to extend the analysis of Ref. [16] to a ring of four mutually coupled van der Pol oscillators with external excitations both in their chaotic and regular states. The purpose of this extension is to find whether our analytical procedure can help to identify or explain at least qualitatively the synchronization states which appear in the excited ring. In the chaotic state, we are limited by the fact that a chaotic orbit is aperiodic and composed of an infinite number of Fourier components. However, we can assume that in the chaotic state, the virtual orbit is that obtained by using the harmonic balance method and therefore defined by the following equation:

$$x_0 = A \cos(\Omega t + \varphi). \quad (2)$$

We note here that this analytical investigation is valid only for identical oscillators and coupling coefficients. Then, in-

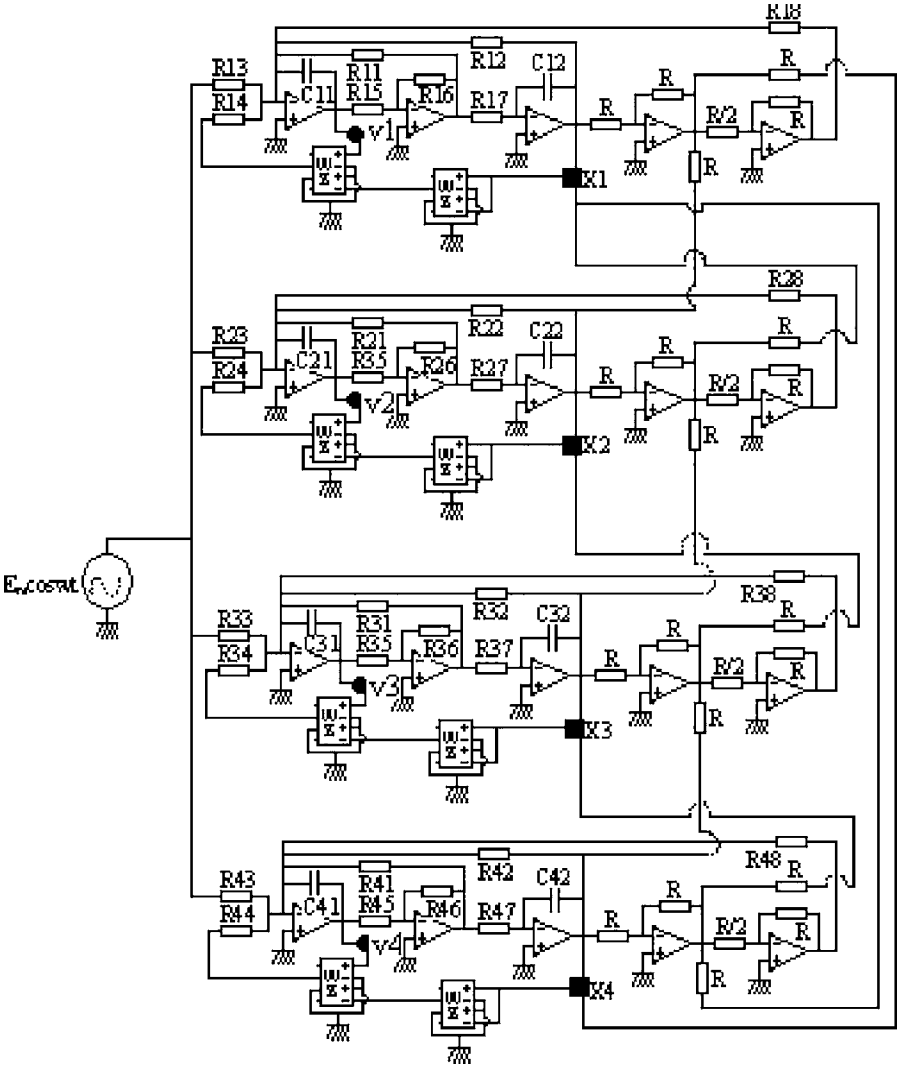

FIG. 3. Circuit of a ring of four mutually coupled van der Pol oscillators using operational amplifiers and multipliers.

serting Eq. (2) into the following Eq. (3) for small values of d:

$$\ddot{x}_0 - d(1 - x_0^2)\dot{x}_0 + x_0 = F\cos(\Omega t), \tag{3}$$

and equating the coefficients of $\sin(\Omega t)$ and $\cos(\Omega t)$ separately, the amplitude A of the oscillatory orbit (virtual orbit in the chaotic state) is the solution of the following algebraic equation:

$$B^3 - 4B^2 + 4(1+\alpha)B - 2\beta = 0, \tag{4}$$

where

$$B = \frac{A^2}{2}, \quad \alpha = \left(\frac{1-\Omega^2}{d\Omega}\right)^2,$$

and

$$\beta = \left(\frac{F}{d\Omega}\right)^2.$$

Let us consider the following parameters: $U = 8 + 72\alpha - 27\beta$ and $V = 1728\alpha(1+\alpha)^2 - 27\beta(144\alpha - 27\beta + 16)$.

If $\alpha \geqslant 1/3$ or if $\alpha \leqslant 1/3$ and $V \geqslant 0$, Eq. (4) has one real solution given by

$$B = \frac{4 - \sqrt[3]{U + \sqrt{V}} - \sqrt[3]{U - \sqrt{V}}}{3}.$$

Whereas if $\alpha \leqslant 1/3$ and $V \leqslant 0$, there are three real solutions given by

$$B_1 = \frac{4}{3}\left[1 - \sqrt{1-3\alpha}\cos\left(\frac{\theta - 2\pi}{3}\right)\right],$$

$$B_2 = \frac{4}{3}\left[1 - \sqrt{1-3\alpha}\cos\left(\frac{\theta}{3}\right)\right],$$

and

$$B_3 = \frac{4}{3}\left[1 - \sqrt{1-3\alpha}\cos\left(\frac{\theta + 2\pi}{3}\right)\right],$$

$$\text{with } \theta = \tan^{-1}\left(\frac{\sqrt{-V}}{U}\right).$$

For identical oscillators, the stability of the dynamical state can be studied through the linearization of Eq. (1) around the unperturbed limit cycle x_0 according to $x_j = x_0 + y_j (1 \leqslant j \leqslant 4)$

TABLE I. Values of capacitors and resistances used in the electronic circuit.

Resistances (Ω) and capacitors (nF)	oscillator-1 ($j=1$)	oscillator-2 ($j=2$)	oscillator-3 ($j=3$)	oscillator-4 ($j=4$)
R_{j1}	9760	9780	9760	9790
R_{j2}	1030	1030	1000	1020
R_{j3}	$0-10^3$	$0-10^3$	$0-10^3$	$0-10^3$
R_{j4}	101	102	100	100
R_{j5}	9780	9800	9810	9780
R_{j6}	9780	9800	9810	9780
R_{j7}	$0-10^5$	$0-10^5$	$0-10^5$	$0-10^5$
R_{j8}	$0-5\times10^7$	$0-5\times10^7$	$0-5\times10^7$	$0-5\times10^7$
R	18×10^4	18×10^4	18×10^4	18×10^4
C_{j1}	12.0	12.5	12.6	12.3
C_{j2}	12.2	12.5	12.6	12.4

where y_j stand for the perturbation variables. If we introduce the rescaling $\tau=\Omega t+\varphi$ and the following diagonal variables z_j as:

$$z_1 = y_1 + y_2 + y_3 + y_4,$$

$$z_2 = y_4 - y_2,$$

$$z_3 = y_3 - y_1,$$

$$z_4 = y_4 - y_3 + y_2 - y_1, \tag{5}$$

we get, after some algebraic manipulations, the following variational equations:

$$\ddot{z}_j + 2[\lambda + f(\tau)]\dot{z}_j + g_j(\tau)z_j = 0, \quad j = 1,2,3,4, \tag{6}$$

with

$$\lambda = -\frac{d}{2\Omega}(1-B),$$

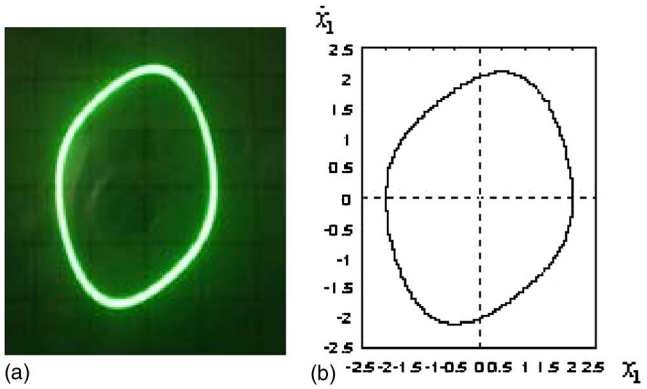

FIG. 4. (Color online) Phase plane of the first oscillator in the regular state (without external excitation) before the coupling; (a) experimentally obtained, (b) numerically obtained.

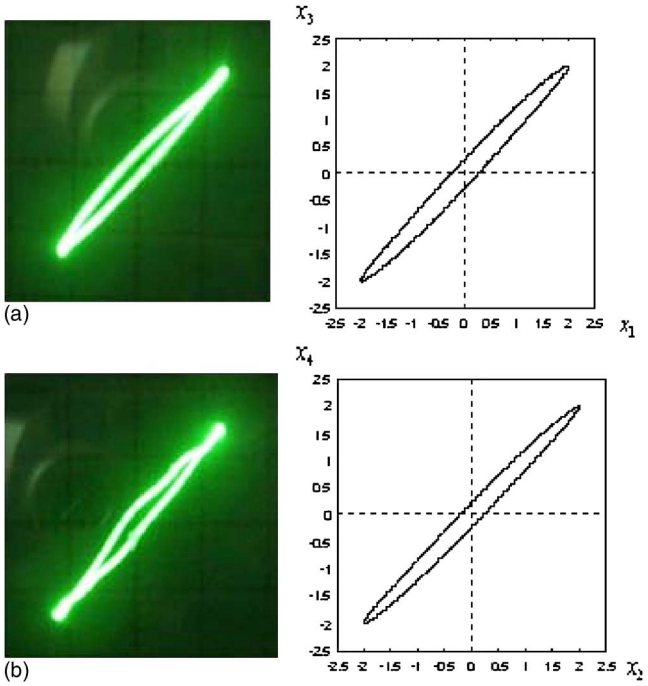

FIG. 5. (Color online) Phase planes showing the absence of synchronization in the ring. Experimental results are shown on the left and numerically simulated plot on the right; (a) x_3 vs x_1, (b) x_4 vs x_2.

$$f(\tau) = \frac{dB}{2\Omega}\cos 2\tau,$$

$$g_1(\tau) = \frac{1}{\Omega^2}(1 - 2dB\Omega \sin 2\tau),$$

$$g_2(\tau) = g_3(\tau) = g_1(\tau) + \frac{2k}{\Omega^2},$$

and

$$g_4(\tau) = g_1(\tau) + \frac{4k}{\Omega^2}.$$

From the expression of $g_j(\tau)$ $j \in [1,4]$, we find that if $k \in [-\infty,-0.25]$, z_j grows with time and the ring is in the state of uncorrelated dynamics. To go further, let us use the following transformation:

$$z_j = \eta_j e^{-\int[\lambda+f(\tau')]d\tau'}. \tag{7}$$

It comes that η_j satisfies the following set of uncoupled Hill equations [20]:

$$\ddot{\eta}_j + (a_{0j} + 2a_{1s}\sin 2\tau + 2a_{1c}\cos 2\tau + 2a_{2c}\cos 4\tau)\eta_j = 0, \tag{8}$$

$$j = 1,2,3,4$$

where

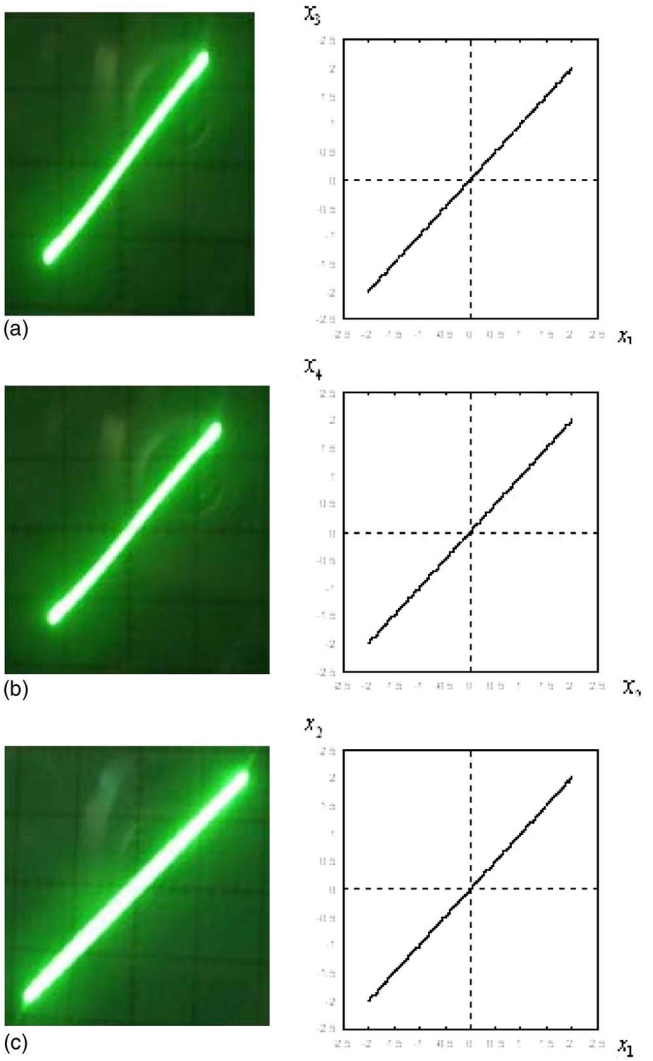

FIG. 6. (Color online) Phase planes of complete synchronization in the system. Experimental results are shown on the left and numerically simulated plot on the right; (a) x_3 vs x_1, (b) x_4 vs x_2, (c) x_2 vs x_1.

$$a_{01} = \frac{1}{\Omega^2}\left[1 - \frac{d^2}{4}(1-B)^2 - \frac{d^2B^2}{8}\right],$$

$$a_{02} = a_{03} = a_{01} + \frac{2k}{\Omega^2}, \quad a_{04} = a_{01} + \frac{4k}{\Omega^2},$$

$$a_{1s} = -\frac{dB}{2\Omega}, \quad a_{1c} = \frac{d^2}{4\Omega^2}(1-B)B, \quad a_{2c} = -\frac{d^2B^2}{16\Omega^2}.$$

The behavior of each z_j depends on the coupling parameter k and we need to determine the range of k for the synchronization process to be achieved. For this aim, we use the Whittaker method [20] to discuss unstable solutions. Thus, we find the solution of Eq. (8) in the form

$$\eta_j = e^{\mu_j \tau}\sin(n\tau - \varphi_j), \tag{9}$$

with μ_j and φ_j being the characteristic exponents and phases respectively. Substituting η_j into Eq. (8) and equating

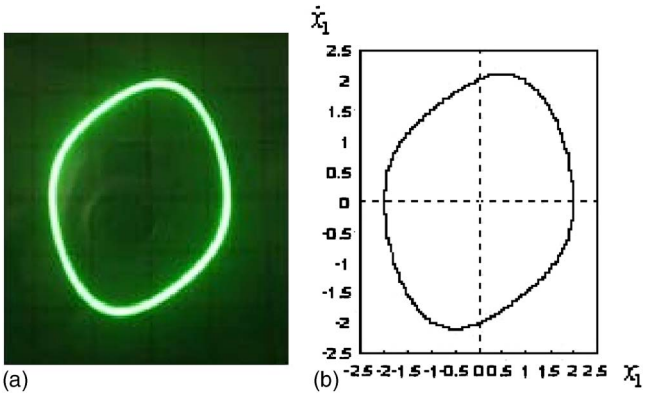

FIG. 7. (Color online) Phase plane of the first oscillator in a complete synchronization in regular state; (a) experimentally obtained, (b) numerically obtained.

the coefficient of $\sin n\tau$ and $\cos n\tau$ separately to zero, we find that the characteristic exponents have the following expressions:

$$\mu_j^2 = -a_{0j} - n^2 + \sqrt{4n^2 a_{0j} + a_n^2}, \quad n = 1,2 \text{ and } j = 1,2,3,4 \tag{10}$$

with $a_n^2 = a_{ns}^2 + a_{nc}^2$.

The synchronization process is stable when the Fourier modes z_j tend to zero with increasing time. Hence the real part of $-\lambda \pm \mu_j$ should be negative. Consequently, the synchronization process is stable under the following conditions:

$$(a_{0j} - n^2)^2 + 2(a_{0j} + n^2)\lambda^2 + \lambda^4 - a_n^2 > 0, \tag{11}$$

$$n = 1,2 \text{ and } j = 1,2,3,4.$$

For $j=1$, the condition (11) is satisfied for all n and for all value of k. The other cases are treated by putting $a_{oj} = \gamma_j k + a_{01}$ $(j=2,3,4)$ where $\gamma_2 = \gamma_3 = 2/\Omega^2$ and $\gamma_4 = 4/\Omega^2$. Equations (11) become

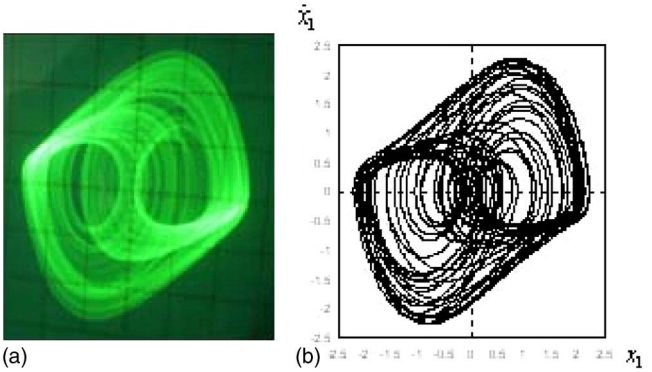

FIG. 8. (Color online) Phase plane of the first oscillator in chaotic state (with external excitation) before the coupling; (a) experimental results (b) numerical results.

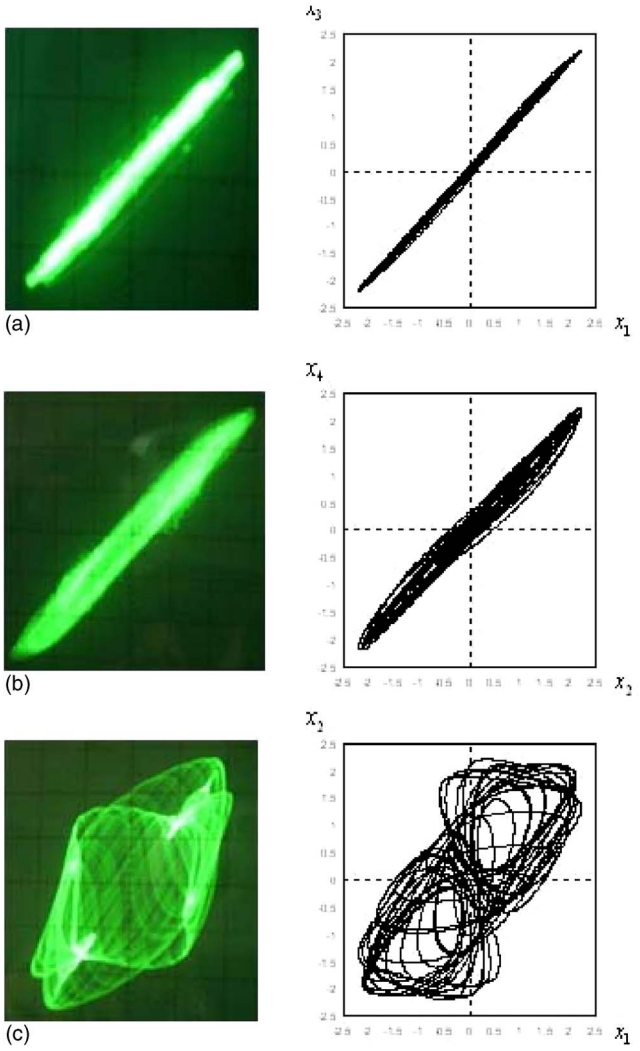

FIG. 9. (Color online) Phase planes illustrating the absence of synchronization in the ring. Experimental results are shown on the left and numerically simulated plot on the right; (a) x_3 vs x_1, (b) x_4 vs x_2, (c) x_2 vs x_1.

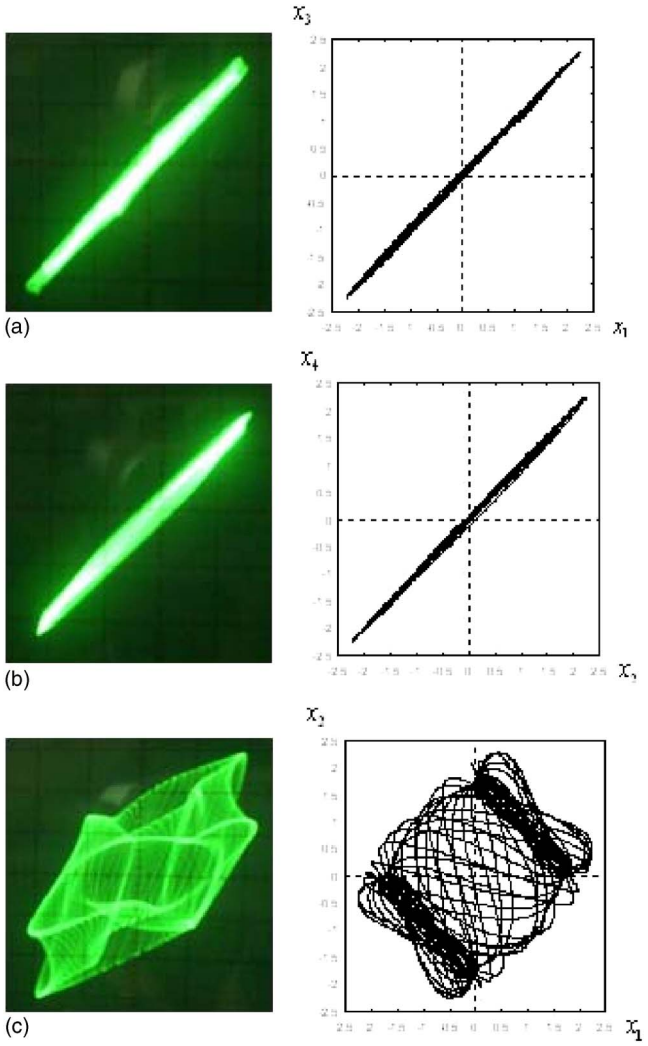

FIG. 10. (Color online) Phase planes illustrating the partial synchronization in the ring. Experimental results are shown on the left and numerically simulated plot on the right; (a) x_3 vs x_1, (b) x_4 vs x_2, (c) x_2 vs x_1.

$$(\gamma_j k)^2 + 2\gamma_j k(a_{01} - n^2 + \lambda^2) + (a_{01} - n^2)^2 + 2(a_{01} + n^2)\lambda^2 - a_n^2 > 0. \tag{12}$$

If $a_n^2 < 4n^2\lambda^2$, Eqs. (12) are satisfied for all values of k. Otherwise we have the following domain of stability (where z_j tend to zero): $k \in [-0.25, k_{10}] \cup [k_{20}, +\infty]$ with

$$k_{10} = \frac{n^2 - a_{01} - \lambda^2 - \sqrt{a_n^2 - 4n^2\lambda^2}}{\gamma_j}$$

and

$$k_{20} = \frac{n^2 - a_{01} - \lambda^2 + \sqrt{a_n^2 - 4n^2\lambda^2}}{\gamma_j}.$$

Figure 2 presents the variation of k_{20} as a function of the amplitude F of the external excitation. The curve in dashed line is the results of the numerical simulation. It is obtained while recording the first value of k for which the three above-stated Fourier modes z_j tend to zero with increasing time. As F increases, the difference between the analytical and numerical results increases. This is understandable since the approximate form (2) assumes small F and d. Nevertheless, the graphs show that the bigger F becomes, the more the complete synchronization appears for relatively large values of the coupling coefficients.

III. EXPERIMENT

A. The experimental setup

The circuit was built according to the scheme shown in Fig. 3 by using TL-082 operational amplifiers and AD-633 multipliers. The TL-082 was used to minimize output drift due to offset and bias current. The values of the resistances and capacitors used are given in Table I. The relations between numerical parameters and those of the circuit are as follows:

$$\omega_{0j} = \sqrt{\frac{R_{j6}}{R_{j2}R_{j5}R_{j7}C_{j1}C_{j2}}}, \quad d_j = \frac{1}{100R_{j4}C_{j1}\omega_{0j}},$$

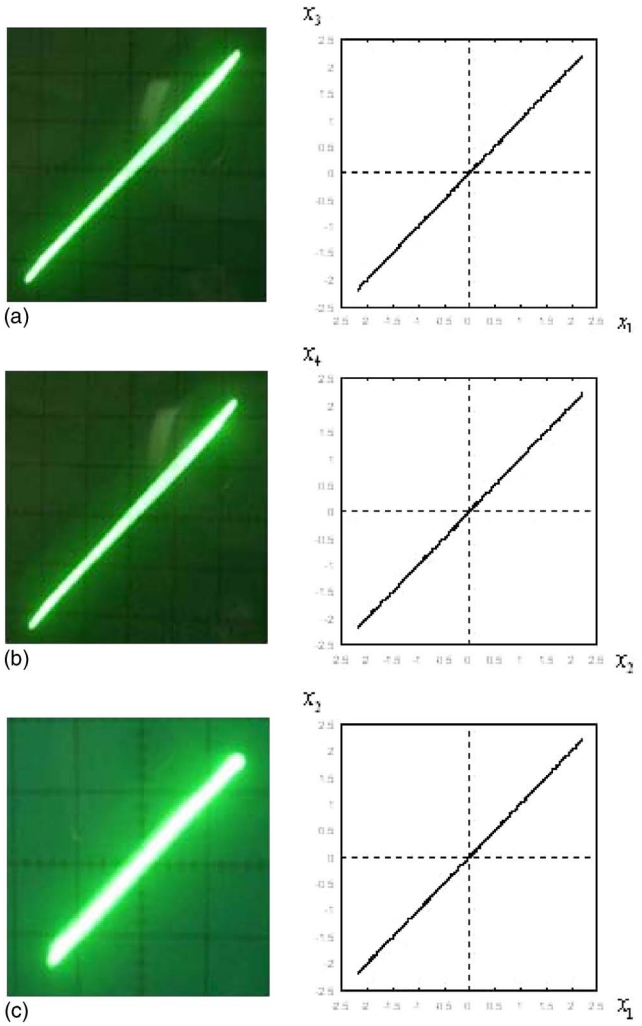

FIG. 11. (Color online) Phase planes illustrating complete synchronization in the ring. Experimental results are shown on the left and numerically simulated plot on the right; (a) x_3 vs x_1, (b) x_4 vs x_2, (c) x_2 vs x_1.

$$F_j = \frac{R_{j2}E_m}{R_{j3}}, \quad \text{and } k_j = \frac{R_{j2}}{R_{j8}}.$$

Using the values in the table, the simplified relations then become

$$d_1 = 3.204 \cdot 10^{-3}\sqrt{R_{17}}, \quad d_2 = 3.146 \cdot 10^{-3}\sqrt{R_{27}},$$

$$d_3 = 3.162 \cdot 10^{-3}\sqrt{R_{37}}, \quad d_4 = 3.200 \cdot 10^{-3}\sqrt{R_{47}},$$

$$F_1 = \frac{1030}{R_{13}}, \quad F_2 = \frac{1030}{R_{23}}, \quad F_3 = \frac{1000}{R_{33}}, \quad F_4 = \frac{1020}{R_{43}},$$

$$k_1 = \frac{1030}{R_{81}}, \quad k_2 = \frac{1030}{R_{82}}, \quad k_3 = \frac{1000}{R_{83}}, \quad k_4 = \frac{1020}{R_{84}}.$$

The quantities x_j in Eqs. (1) are the voltage of the jth oscillator as indicated in Fig. 3, while v_j, also indicated, are the points for the first time derivative of the potentials.

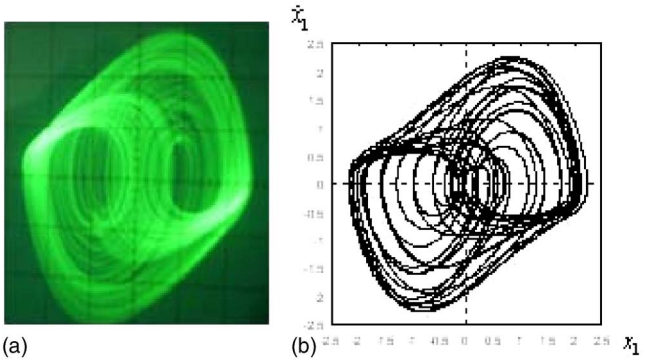

FIG. 12. (Color online) Phase plane of the first oscillator when the ring is in the complete synchronization state; (a) experimentally obtained, (b) numerically obtained.

B. Synchronization in the autonomous ring

We set $E_m=0$ and use the resistances R_{j7} (e.g., d_j) as the controlling parameters. Varying R_{j7} in the same way, we find different configurations. Figure 4(a) shows the phase plane of the first oscillator obtained for $R_{17}=9.97$ kΩ when there is no coupling. Its numerical analogue [Fig. 4(b)] is given for $d_1=0.32$. After setting the coupling ($R_{17}=9.97$ kΩ, $R_{27}=10.22$ kΩ, $R_{37}=10.31$ kΩ, $R_{47}=9.88$ kΩ), we decrease the values of the resistances R_{j8}, (e.g., k_j) and find that for $0.25\ \text{MΩ} \leqslant R_{j8} \leqslant 50\ \text{MΩ}$, there is no synchronization state in the ring. This can be appreciated in Figs. 5(a) and 5(b) and drawn for $R_{18}=34.3$ MΩ, $R_{28}=33.2$ MΩ, $R_{38}=33.4$ MΩ, and $R_{48}=32.9$ MΩ, thus $k_1=3\times10^{-5}$, $k_2=3.1\times10^{-5}$, $k_3=2.99\times10^{-5}$, and $k_4=3.14\times10^{-5}$, respectively. Figure 6 illustrates the complete synchronization state of the ring for $R_{18}=204.8$ Ω, $R_{28}=205$ Ω, $R_{38}=200.5$ Ω, $R_{48}=202.5$ Ω, and $k_1=5.03$, $k_2=5.025$, $k_3=5.027$, $k_4=5.031$. Figures 7(a) and 7(b) show the phase plane of the first oscillator during a complete synchronization.

C. Synchronization in the periodically excited ring

Here, we fix $E_m=0.5$ V, $\Omega=0.35$ Hz, and proceed as in the Sec. III B. Figure 8 shows the phase plane of the first oscillator before the coupling. For the investigation of synchronized states, we use the following values of the electrical components: $R_{17}=37.4$ kΩ, $R_{27}=38.7$ kΩ, $R_{37}=38.6$ kΩ, $R_{47}=37.5$ kΩ, $R_{13}=504$ Ω, $R_{23}=505$ Ω, $R_{33}=490$ Ω, and $R_{43}=500$ Ω. This corresponds to $d_1=0.62$, $d_2=0.619$, $d_3=0.621$, $d_4=0.62$, $F_1=1.021$, $F_2=1.019$, $F_3=1.02$, and $F_4=1.019$ for the numerical simulations.

In addition to the observations in the Sec. III B, it is necessary to mention that after the system synchronizes for a combination of values, if one decreases the resistances R_{j3} in order to come out of synchronization, then one cannot fall again in the synchronization unless the resistances R_{j7} are decreased. Therefore, for small values of R_{j3} (large values of F_j), the system begins to synchronize for small values of R_{j7} (large values of k_j). This corresponds to what has been foreseen from the theoretical investigation. Here, if $50\ \text{MΩ} \geqslant R_{j8} \geqslant 0.17\ M\Omega$, there is no synchronization in the ring. Figure 9 shows different phase planes of the system

out of the synchronization. The parameters used are the following: $R_{18}=5.35\ \mathrm{M}\Omega$, $R_{28}=4.92\ \mathrm{M}\Omega$, $R_{38}=4.87\ \mathrm{M}\Omega$, $R_{48}=5.10\ \mathrm{M}\Omega$, and thus $k_1=2\times10^{-4}$, $k_2=2.1\times10^{-4}$, $k_3=2.2\times10^{-4}$, $k_4=2\times10^{-4}$. Figures 10 and 11 highlight the case of partial synchronization and complete synchronization respectively. Figure 10 is obtained for $R_{18}=6.02\ \mathrm{k}\Omega$, $R_{28}=6.09\ \mathrm{k}\Omega$, $R_{38}=5.88\ \mathrm{k}\Omega$, and $R_{48}=6.00\ \mathrm{k}\Omega$ (thus $k_1=0.171$, $k_2=0.169$, $k_3=0.173$, and $k_4=0.17$). Figure 11 is plotted for $R_{18}=1.20\ \mathrm{k}\Omega$, $R_{28}=1.17\ \mathrm{k}\Omega$, $R_{18}=1.16\ \mathrm{k}\Omega$, and $R_{48}=1.17\ \mathrm{k}\Omega$ (thus $k_1=0.874$, $k_2=0.879$, $k_3=0.873$, and $k_4=0.875$). Figure 12 shows that in the complete synchronization state of Fig. 11, the oscillators are in the chaotic state.

IV. CONCLUSION

In this paper, we have investigated different states of synchronization in a ring of four mutually coupled van der Pol oscillators both in their regular and chaotic states. The Whittaker method has helped us to obtain the boundaries of the synchronization process when the external force is present. We have found a fairly good agreement between the theoretical and experimental results, specifically in cases of weak nonlinear coefficients and small parameters mismatch. It has been shown in our analysis that the accuracy of synchronization becomes reliable for large coupling parameters.

For further investigations, several important issues remain open. For instance, other coupling schemes can be considered and an extension to more than four oscillators is interesting as it can improve our understanding of large network constituted of self-sustained oscillators, e.g., multipeds. Another point of interest is the consideration of time delay between the dynamics of oscillators. Indeed, in the network, the signal processing can be effected in such a way that an oscillator reacts to the signal of its neighbors after a time delay.

ACKNOWLEDGMENTS

This work is supported by the Academy of Sciences for the Developing World (TWAS) under Research Grant No. 03-322 RG/PHYS/AF/AC. P. Woafo acknowledges support from the Swedish International Development Agency.

[1] L. M. Pecora and T. L. Carroll, Phys. Rev. Lett. **64**, 821 (1990).
[2] N. F. Rulkov, M. M. Sushchik, L. S. Tsimring, and H. D. I. Abarbanel, Phys. Rev. E **51**, 980 (1995).
[3] R. Fermat and J. Alvarez-Ramirez, Phys. Lett. A **236**, 307 (1997).
[4] N. J. Corron and D. W. Hahs, IEEE Trans. Circuits Syst., I: Fundam. Theory Appl. **44**, 373 (1997).
[5] Y. Zhang, G. Hu, H. A. Cerdeira, S. Chen, T. Braun, and Y. Yao, Phys. Rev. E **63**, 026211 (2001).
[6] B. Mensour and A. Longtin, Phys. Lett. A **59**, 244 (1998).
[7] P. Woafo, Phys. Lett. A **31**, 267 (2000).
[8] J. Collins and I. Stewart, J. Nonlinear Sci. **3**, 349 (1993).
[9] M. Golubitsky, I. Stewart, P-L. Buono, and J. J. Collins, Physica D **115**, 56 (1993).
[10] M. Golubitsky, I. Stewart, P-L. Buono, and J. J. Collins, Nature **401**, 693 (1999).
[11] P-L. Buono and M. Golubitsky, J. Math. Biol. **42**, 291 (2001).
[12] P-L. Buono, M. Golubitsky, and A. Palacio, Physica D **143**, 74 (2000).
[13] H. Castellini, E. Yudiarsah, L. Romanelli, and H. A. Cerdeira, Pramana **64**, 525 (2005).
[14] S. Boccaletti, J. Kurths, G. Osipov, D. L. Valladares, and C. S. Zhou, Phys. Rep. **366**, 1 (2002).
[15] T. Ookawara and T. Endo, IEEE Trans. Circuits Syst., I: Fundam. Theory Appl. **46**, 827 (1999).
[16] P. Woafo and H. G. Enjieu Kadji, Phys. Rev. E **69**, 046206 (2004).
[17] S. H. Strogatz, *Nonlinear Dynamics and Chaos: With Applications in Physics, Biology, Chemistry, and Engineering* (Addition-Wesley, New York, 1994).
[18] I. A. Heisler, T. Braun, Y. Zhang, G. Hu, and H. A. Cerdeira, Chaos **13**, 185 (2003).
[19] J. D. Murray, *Mathematical Biology* (Springer, New York, 1989).
[20] C. Hayashi, *Nonlinear Oscillations in Physical Systems* (McGraw Hill, New York, 1964).